

On determining the cluster abundance normalization

Elena Pierpaoli¹, Stefano Borgani², Douglas Scott³ and Martin White⁴

¹*Physics and Astronomy Department, Princeton University, Princeton, NJ, 08544 USA*

²*Dipartimento di Astronomia, Università di Trieste, via Tiepolo 11, I-34131 Trieste Italy*

³*Department of Physics and Astronomy, University of British Columbia, Vancouver, B.C., V6T 1Z1 Canada*

⁴*Departments of Physics and Astronomy, University of California, Berkeley, CA, 94720 USA*

Accepted ... ; Received ... ; in original form ...

ABSTRACT

Different determinations currently suggest scattered values for the power spectrum normalization on the scale of galaxy clusters, σ_8 . Here we concentrate on the constraints coming from the X-ray temperature and luminosity functions (XTF and XLF), and investigate several possible sources of discrepancies in the results. We conclude that the main source of error in both methods is the scaling relation involved, in particular the way its intrinsic scatter and systematic normalization are treated.

For temperature derived constraints, we use a sample adapted from HIFLUGCS, and test for several sources of systematic error. We parameterize the mass-temperature relation with an overall factor T_* , which varies between about 1.5 and 1.9 in the literature, with simulations typically giving lower results than empirically derived estimates. After marginalising over this range of T_* , we obtain a 68 per cent confidence range of $\sigma_8 = 0.77^{+0.05}_{-0.04}$ for a standard Λ CDM model.

For luminosity derived constraints we use the XLF from the REFLEX survey and explore how sensitive the final results are on the details of the mass–luminosity, M – L , conversion. Assuming a uniform systematic uncertainty of ± 20 per cent in the amplitude of the mass-luminosity relation by Reiprich & Böhringer, we derive $\sigma_8 = 0.79^{+0.06}_{-0.07}$ for the same standard Λ CDM model. Although the XTF and XLF derived constraints agree very well with each other, we emphasize that such results can change by about 10–15 per cent, depending on how uncertainties in the L – T – M conversions are interpreted and included in the analysis.

We point out that in order to achieve precision cosmology on σ_8 using cluster abundance, it is first important to separate the uncertainty in the scaling relation into its intrinsic and overall normalization parts. Careful consideration of all sources of scatter is also important, as is the use of the most accurate formulae and full consideration of dependence on cosmology. A significant improvement will require the simultaneous determination of mass using a variety of distinct methods, such as X-ray observations, weak lensing, Sunyaev-Zel’dovich measurements and velocity dispersions of member galaxies, for a moderately large sample of clusters.

Key words: gravitation – galaxies: clusters: general – cosmology: theory – large-scale structure of Universe

1 INTRODUCTION

The normalization of density perturbations on large scales is a fundamental parameter describing our Universe. Its determination has been actively pursued for the last quarter century, using a wide range of methods. Now we are entering the era of precision cosmology, with several cosmological parameters apparently determined to better than 10 per cent accuracy. While this level of precision has been reached for the amplitude of the largest scale perturbations, through the

COBE anisotropy measurements, the direct normalization of matter fluctuations on galaxy cluster scales still yields a wide range of estimates.

Here we focus on the determination of the cluster mass distribution via X-ray observations, and discuss how differences in the details of the adopted strategies can lead to different, sometimes quite discrepant, determinations of σ_8 . While considering X-ray observations, two approaches have traditionally been adopted. The first one is based on determining the cluster X-ray luminosity function (XLF) and

then converting it into the mass function through a suitable Mass–Luminosity, M – L , conversion (e.g. Henry et al. 1992; Sadat, Blanchard & Oukbir 1998; Reichart et al. 1999; Borgani et al. 2001; Reiprich & Böhringer 2002; Viana, Nichol & Liddle 2002; Schuecker et al. 2002). The second possibility is to use measurements of the X-ray temperature function (XTF) and then apply a Mass–Temperature, M – T , relation (e.g. Oukbir & Blanchard 1992; Eke et al. 1998; Viana & Liddle 1998; Pen 1998; Markevitch 1998; Pierpaoli, Scott & White 2001; Seljak 2002).

Measuring cluster luminosities requires ~ 10 times less X-ray photons than measuring temperature. This has allowed us to precisely determine the XLF for samples containing a few hundreds of local clusters. Current independent determinations of the XLF agree with each other at high precision (see Rosati, Borgani & Norman 2002, for a review), thus making it a stable reference point to quantify the cluster population. However, the dependence of the bremsstrahlung emissivity on the square of the local gas density causes the X-ray luminosity to be highly sensitive to the core and to local details of the intra-cluster medium (ICM) structure. This makes it a noisy and difficult to calibrate mass estimator. Resorting to an observationally calibrated M – L relation is in principle possible through two alternative routes: either combining the L – T and the M – T relations, or directly measuring an M – L scaling. Both approaches require an independent measure of M , which is a notoriously difficult problem. Traditionally, masses are estimated either by applying hydrostatic equilibrium to a cluster with a measured temperature pattern and surface brightness profile (Reiprich & Böhringer 2002; Ettori, De Grandi & Molendi 2002), or using the mass estimated through cosmic shear (e.g. Viana & Liddle 2002, Allen et al. 2002). Both of these methods could suffer biases (Evrard, Metzler & Navarro 1996; Metzler, White & Loken 2001) which need to be accounted for.

X-ray temperatures are in principle easier to understand: since the ICM temperature is mainly determined by gravitational processes, it should be more directly related to the total gravitating mass of the cluster, i.e. the M – T relation should have less scatter and be more tractable theoretically. Although this is true to a first approximation, the simplest expectation based on hydrostatic equilibrium and isothermal gas have been shown to provide a poor representation of the observed M – T relation (e.g. Finoguenov et al. 2001; Allen, Schmidt & Fabian 2001). In the absence of improved theoretical modeling one is forced to rely on an empirical calibration of the M – T relation, which raises many of the same issues as for the M – L relation discussed above.

In general, all methods of mass estimation have both a significant scatter and potential systematic errors, leading to discrepant σ_8 results.

For example, Pierpaoli, Scott & White (2001, hereafter PSW) explored several improvements in determining σ_8 from the distribution of local cluster temperatures, using a combination of X-ray data, cluster simulations and theoretical modeling. For $\Omega_m = 0.3$, they constrained the power spectrum normalization to lie around $\sigma_8 \simeq 1$, but stressed how existing uncertainties, particularly in the Mass–Temperature relation, dominate the error bar.

Borgani et al. (2001; hereafter B01, see also Rosati et al. 2002) analyzed the luminosity distribution for the

ROSAT Deep Cluster Survey out to $z \sim 1$. They paid particular attention to the impact of uncertainties and scatter in the M – L conversion on the final results. They preferred a lower normalization, $\sigma_8 \simeq 0.7$ for $\Omega_m = 0.3$, with a roughly 15 per cent uncertainty mainly driven by the systematics affecting the M – L relation.

In this paper we use the local XLF from the REFLEX survey (Böhringer et al. 2002) and the distribution of temperatures from a new compilation of nearby clusters

based on HIFLUGCS (Reiprich & Böhringer 2002). Besides providing further constraints on σ_8 , we will discuss how these two different approaches to the cluster mass function are affected by systematics, and under which conditions they provide consistent constraints on cosmological parameters. Our basic conclusion will be that the two approaches in fact give consistent results, although at present it is not realistic to expect a determination of σ_8 to better than 10 per cent.

More specifically, after giving the theoretical frame (Section 2), we analyze the temperature-derived constraint in Section 3. We assess several possible different sources of error, including: the M – T normalization and its scaling; the effect of the L – T normalization error on the computation of the effective volume; different temperature determinations; and different cuts of the data. For luminosity-derived constraints, in Section 4 we compare the results obtained from the local REFLEX sample with the RDCS, therefore testing possible evolutionary effects. We also compare results obtained by applying the direct L – M relation with those obtained via the the L – T – M approach. In the end, we also compare the luminosity- and temperature-derived constraints. We thoroughly discuss how error treatments can influence the final result throughout, particularly in Section 5, where we also compare our results to other recent determinations of σ_8 . Finally, we present our conclusions in Section 6.

2 THEORY

The mass variance is constrained from the cluster abundance through the mass function – the (comoving) number density of objects of a specified mass. While there has been significant progress in the theory of the mass function of late, there still remain serious systematic uncertainties in the theoretical predictions, and it is therefore important to specify which expression for the the mass function is being adopted. Jenkins et al. (2001) used a variety of N -body simulations for different cosmological models to derive analytic expressions for the mass function of dark matter halos. In particular, the expression in their equation (B3),

$$\frac{dn}{dM} = 0.301 \frac{\bar{\rho}}{M^2} \frac{d \ln \sigma^{-1}}{d \ln M} \exp(-|\ln \sigma^{-1} + 0.64|^{3.82}), \quad (1)$$

has been shown to reproduce the distribution of halos, if the mass is interpreted as that within the radius, r_{180m} , interior to which the mean overdensity is $\rho = 180\bar{\rho}_m$, for their ‘ τ CDM’ simulation. Here $\bar{\rho}_m$ is the ‘background’ density or the mean cosmic mass density (i.e. Ω_m times the critical density). They also show that the mass function is approximately ‘universal’ if the mass is taken to be the sum of the particles found in their simulation with a particular group finder. The combination of these findings strongly suggests

that equation (1) describes the mass function for a wide range of theories if the mass is measured interior to r_{180m} (see also Hu & Kravtsov 2002; White 2002).

Jenkins et al. (2001) have confirmed and extended earlier work which shows that the standard Press–Schechter expression for the mass function (Press & Schechter 1974) significantly overestimates and underestimates the number density of halos in the low- and high-mass end of their distribution, respectively (see also Evrard et al. 2002). They also found that the mass-function by Sheth & Tormen (1999) somewhat overestimates the number density of very massive halos, although this difference is probably negligible for our current purposes. However, in general, different expression for the mass functions induce differences of 4–8 per cent in the resulting value of σ_8 , which are comparable to or larger than the statistical uncertainties.

In addition to this, Jenkins et al. (2001) and White (2002) have shown that the mass function is not precisely a universal function, i.e. it is not simply a function of the linear density field smoothed on an appropriate scale. While different cosmologies predict mass functions which are very similar, in scaled units, there is a ‘scatter’ of several tens of per cent in number at fixed mass. The non-universality of the mass function introduces an additional, and non-negligible, systematic uncertainty in the conversion between a measured object’s abundance and the cosmological parameters. As we push to more precise estimates of increasing numbers of parameters these issues will need to be confronted head on. However, for the moment we shall ignore such refinements as our focus will be on currently more important systematic errors.

The mass entering in equation (1) should be interpreted as the mass contained within r_{180m} , i.e. inside a radius encompassing a mean overdensity $\rho = 180\bar{\rho}_m$. However, scaling relations connecting mass to X-ray observable quantities may provide the mass at different values of $\rho/\bar{\rho}$ (see below). In this case we follow White (2001) and rescale the masses assuming an NFW profile for the DM halo (Navarro, Frenk & White 1996) with a concentration $c = 5$ appropriate for a rich cluster. A similar procedure by Hu & Kravtsov (2002) gives essentially identical results.

The quantity $\sigma(M, z)$ in equation (1) describes the perturbation of the mass-scale M , which is the mass contained within a top-hat sphere of comoving radius R , such that $M = (4\pi/3)\bar{\rho}R^3$. In terms of the power spectrum, it is

$$\sigma^2(R, z) = \int_0^\infty \frac{dk}{k} \Delta^2(k, z) W^2(kR), \quad (2)$$

where $\Delta^2 = k^3 P(k, z)/(2\pi^2)$, $P(k) \equiv |\delta_k|^2 \propto k^n T^2(k)$ is the matter power spectrum ($n = 1$ will be assumed in the following for the primordial spectral index), $W(kR)$ is the window function corresponding to the smoothing of the density field (the Fourier transform of a top-hat in this case) and $T(k)$ is the transfer function. For the latter we use the fitting expression provided by Eisenstein & Hu (1999).

We notice here that such commonly used approximations for σ_8 or for the transfer function may introduce systematic sources of error. For example, the Viana & Liddle fitting formula for σ_8 as a function of cosmology is imprecise at the level of 2–3 per cent for Ω_m values as low as 0.2. Another common choice is the use of the Bardeen et al. (1986) fitting formula with no baryons in conjunction

with an expression for the ‘shape parameter’ Γ which models the baryon dependence. This can introduce differences in the transfer function of 5–20 per cent around $k \simeq 0.1 h \text{ Mpc}^{-1}$. We will stick with the Jenkins et al. (2001) mass function and the transfer function given by Eisenstein & Hu (1999).

In carrying out these comparisons, we restrict ourselves to flat cosmological models with an initial power spectrum index of $n = 1$, and pure cosmological constant making up the dark energy. We will also fix the baryon fraction to be $\Omega_b h^2 = 0.02$, and either allow Ω_m to be free, or fix its value at 0.3. Scaling relations for other cosmologies can be found in PSW.

Once one has adopted a cosmology and a mass function, then the power spectrum can be normalized using some property of the clusters which can be used to estimate mass. For studies which focus on the X-ray properties of clusters, then all methods effectively use either the X-ray temperature function (XTF) or the X-ray luminosity function (XLF).

3 CONSTRAINTS FROM THE XTF

In this section we present our σ_8 determination derived from the temperature measurements. We first discuss the sample used (Section 3.1), then the possible choices for temperature modeling (Section 3.2), the M – T scaling relation (Section 3.3), our methodology (Section 3.4), and finally the results (Section 3.5).

3.1 The local sample

Since almost all recently used cluster samples derive from essentially the same *ROSAT* databases, it is intriguing that different selections and treatment of the data apparently give such different results. It is therefore clearly important to define one’s sample as carefully as possible.

The error bars on σ_8 are not dominated by Poisson fluctuations in the small number of sources, but by systematic sources of scatter. So it is important to have a well understood cluster sample, rather than the largest available one. We specifically focus on a *local sample*, by which we mean clusters with red shift $z \leq 0.1$. This allows us to avoid evolution issues. We also exclude the nearest clusters (at $z < 0.03$) to avoid possible biases introduced by survey incompleteness and local super-clustering.

In PSW we defined a cluster catalogue adapted from the approach of Markevitch (1998), which was based on *ROSAT*-selected clusters with *ASCA*-derived temperatures. Our temperatures there were taken from White (2000), who fitted *ASCA* data with a model which included the effects of cooling flows. We supplemented these cooling-flow corrected temperatures with a few temperature estimates drawn from the literature. Since that work the available X-ray catalogues have improved significantly.

The HIFLUGCS catalogue (Reiprich & Böhringer 2002) has now been published, and is probably the most complete publicly available X-ray catalogue based on the *ROSAT* All Sky Survey (RASS, Trümper et al. 1990). Reiprich & Böhringer (2002, hereafter RB02) discuss the selection of the HIFLUGCS sample in detail. Here we give the most relevant features only. The main selection criterion is a flux threshold at $1.7 \times 10^{-14} \text{ W m}^{-2}$ in the *ROSAT* 0.1–2.4 keV

band. The final flux limit is set at $f_{\text{lim}} = 2.0 \times 10^{-14} \text{ W m}^{-2}$, above which it appears the sample is very close to complete over the 8.14 sr it covers. This sample contains 63 clusters, with an additional 43 clusters in an extended list. Rather than use the ASCA derived, cooling flow corrected temperatures from White (2000), we have used the temperatures quoted by Ikebe et al. (2002). They present temperatures for the HIFLUGCS clusters determined from a two-temperature fit.

In constructing our sample we exclude both the nearest ($z < 0.03$) and most distant ($z > 0.1$) clusters, to avoid possible biases. Within these limits we wish to construct an effectively temperature limited sample, so we need to adopt a relation between X-ray temperature and luminosity. The luminosity-temperature relation for HIFLUGCS is (Ikebe et al. 2002, equation (4))

$$L = (1.38 \times 10^{35}) T^{2.5} h^{-2} \text{ W}, \quad (3)$$

with T measured in keV and L in the 0.1–2.4 keV energy band.

We include a cluster if it would have passed the flux cut had its luminosity been given by $L(T)$ and if it is hotter than 3 keV. The errors on the measured temperature are included by weighting each cluster based on the probability it is in the sample assuming a Gaussian distribution of temperatures described by the observed central temperature and error.

While we use the mean L – T relation to compute the weight of each cluster, when we later compute the effective distance to which a cluster of temperature T could have been seen, we include the effect of scatter in L – T (which slightly reduces the distance).

In the following we will use the primary HIFLUGCS sample (63 clusters) as the reference one, but we will also compare the results derived using the PSW catalog (72 clusters) and an extended version of the HIFLUGCS sample which contains 96 clusters from a combination of the extended HIFLUGCS and PSW. Note that after applying the selection criteria presented above, the actual number of clusters used to determine σ_8 is significantly lower (see Section 3.5).

3.2 Modeling cluster temperatures

Authors differ in what they mean by cluster ‘temperature’ and there are a number of subjective choices which can be possible sources of discrepancy, including: different models for fitting T ; varying fields of view and spatial resolutions; spectral band differences; and methods for dealing with sub-structure, modeling mergers, etc. The basic point is that the quoted errors do not include all of the systematic effects and care must be taken to avoid comparing apples with oranges.

A particular difficulty is deciding how to deal with radial structure, particularly in the cluster center. Clearly some procedure needs to be adopted, since a single isothermal model does not adequately fit both the central and outer regions of many clusters. So long as the same procedure is adopted for the method used to fix the M – T normalization as is used for the data, it probably makes little difference precisely what is done. However this is rarely the case in practice. In PSW, for example, we used temperatures from White (2000) which came from a specific cooling flow model which

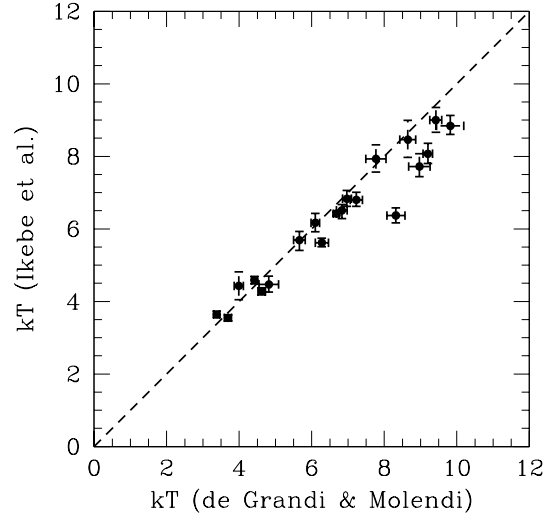


Figure 1. Ikebe et al. (2002) isothermal temperature fits from ASCA data compared with de Grandi & Molendi (2001) temperatures derived from *Beppo-SAX* data for those clusters in common. This is indicative of the current size of systematic errors in temperature estimates.

had been fitted to ASCA data, while Markevitch (1998) simply excised the centres of clusters. The justification for this is that most simulations possess neither the resolution nor the physics to adequately model cooling flows, and hence they should not be allowed to affect the data either.

Recently Ikebe et al. (2002) performed a different fitting for the temperatures of the clusters. They use a 2-temperature picture, in which the outer regions are modeled by a single temperature isothermal plasma, while in the central regions there is a second cooler component forming a multi-phase plasma with the first. For some clusters, with no statistical measurement of a cooler component, they fixed its temperature at $T_{\text{hot}}/2$. They argue that overall this method provides a reasonable description for both cooling-flow and non-cooling-flow clusters. We will therefore use the temperature of the hot isothermal gas as the mass proxy for each cluster in our sample. It is worth pointing out that the temperatures derived using this method are typically lower than those obtained by some previous authors (see fig. 1 in Ikebe et al. 2002); in particular, the discrepancy is bigger for hotter clusters. For clusters hotter than 6 keV, the White (2000) temperatures are approximately 25 per cent hotter than those of Ikebe et al. (2002). It now seems likely that the White (2000) temperatures were overestimated in several cases.

However, to further illustrate this issue we plot in Fig. 1 a comparison of Ikebe et al. (2002) temperatures with those which are in common with a study of clusters using *Beppo-SAX* data by de Grandi & Molendi (2002). Firstly, it is clear that these entirely independent determinations of temperature are in rather good agreement. However, in detail there are differences for individual clusters, and a general trend for the Ikebe et al. (2002) temperatures to be cooler for the highest T objects. This comparison should serve as a useful

guide to the size of possible systematic effects in the temperature determinations. We will later consider the effect on our σ_8 estimate of boosting the temperatures of the highest temperature clusters.

In the following we will adopt temperatures from Ikebe et al. (2002) whenever available, that is for the main HIFLUGCS sample, and the HIFLUGCS extended sample, while we adopt temperatures from PSW for the PSW sample and for the clusters in that supplementary sample.

3.3 The Mass–Temperature relation

The M – T relation is generally assumed to be:

$$\left(\frac{M(T, z)}{10^{15} h^{-1} M_{\odot}} \right) = \left(\frac{T}{T_{*}} \right)^{3/2} (\Delta_c E^2)^{-1/2} \times \left(1 - 2 \frac{\Omega_{\Lambda}(z)}{\Delta_c} \right)^{-3/2}, \quad (4)$$

where T is in keV^{*}, Δ_c is the mean overdensity inside the virial radius in units of the critical density and $E^2 = \Omega_m(1+z)^3 + \Omega_{\Lambda} + \Omega_k(1+z)^2$. Note that Δ_c depends on cosmology, with fitting formulae given in PSW, and is a redshift dependent variable, which should be evaluated using the appropriate $\Omega_{\Lambda}(z)$ and $\Omega_m(z)$.

While equation (4) comes from rather simplistic arguments (essentially dimensional analysis and an assumption that clusters are self-similar) both observations and simulations suggest it is a good approximation for systems hotter than about 3 keV. For example Finoguenov et al. (2001) find

$$M_{500} = (4.22^{+0.85}_{-0.66}) \times 10^{13} h_{50}^{-1} M_{\odot} \times kT^{1.48^{+0.10}_{-0.12}}, \quad (5)$$

for $kT > 3$ keV clusters, where M_{500} is the mass within an overdensity of 500 with respect to critical. Other recent determinations are also consistent with a slope of 1.5 (e.g. Allen et al. 2001; Xu et al. 2001) provided that only the higher temperature clusters are considered.

Unfortunately the level of agreement on the overall normalization, T_{*} , is not so good (see e.g. Table 1 of Muanwong et al. 2002 or fig. 2 of Huterer & White 2002). In fact the uncertainty in T_{*} has for some time been the dominant uncertainty in determining σ_8 . In PSW T_{*} was assumed to be 1.3, in B01 it was assumed to be 1.2. These values are representative of the older simulation results. The observations have almost always suggested a lower normalization for the M – T relation than implied by the theoretical model (i.e. a higher value of T_{*}), which therefore leads to a lower σ_8 value. A rough scaling argument suggests (Huterer & White 2002, see also Fig. 2)

$$\Omega_m^{0.6} \sigma_8 \propto (T_{*})^{-0.8}, \quad (6)$$

with a slightly weaker dependence if only the most massive clusters are used in the analysis (Evrard et al. 2002). Including additional physics in the simulations and trying to

* In PSW we called this normalization β , following some of the simulation papers. However, this caused some confusion because a different subset of authors (motivated by the isothermal β model) have defined a β which is inversely proportional. In addition β is often used to denote the outer slope of the emission profile of clusters. Defining T_{*} in this way is much less ambiguous.

estimate the mass in the same way as the observers helps to reconcile the discrepant normalizations (e.g. Muanwong et al. 2002) and suggests that T_{*} may be closer to 1.6 than the values assumed earlier. Some direct observational determinations (which estimate the mass in different ways) suggest an even higher value (Finoguenov et al. 2001, Xu et al. 2001).

We would like to stress that there are two kinds of uncertainty in the M – T relation: an intrinsic scatter in the temperatures of clusters of a given mass which arises due to differences in their formation history; and an overall uncertainty in the normalization of the M – T relation. The first sort of uncertainty is entirely statistical in character. It needs to be considered, because it both moves the central value for σ_8 and contributes to the error bar. Taking this scatter into account is straightforward if its distribution is known. Most studies have agreed that the scatter is around 10–15 per cent in T , and is essentially a reflection of the different merging histories. The second sort of uncertainty is entirely systematic, however, and has to be treated in a different way, for example by marginalising the likelihood of σ_8 over some prior distribution of values of T_{*} . This distinction is not typically made in determinations of σ_8 from X-ray data.

It is very easy for errors in the determination of T_{*} to creep in. Recall that we are ultimately interested in determining the mass within a sphere of radius r_{180m} centered on the cluster in order to compare to theoretical mass functions. For a typical rich cluster $r_{180m} \simeq 2 - 3 h^{-1}$ Mpc, well beyond the region where observations probe directly, with the possible exception of lensing studies.

In order to determine this mass we may estimate M_{Δ} at one of various different density contrasts Δ using a variety of methods each known to have biases. Assuming an NFW profile with a constant concentration ($c = 5$ is assumed for cluster scale halos) and a flat cosmology with $\Omega_m = 0.3$, then some commonly used masses are related by $M_{\text{vir}} \equiv M_{\Delta_c} = 1.22 M_{200}$, and $M_{500} = 0.72 M_{200}$, while $\Delta_c \simeq 100$. Hence we can derive $M_{\text{vir}} = 1.69 M_{500}$, so the M – T relation of equation (5) implies a normalization of $T_{*} \simeq 1.9$. Significant corrections are being applied in these conversions, involving large extrapolations from given profiles, indicating that there is plenty of room for error.

We caution that there is also a significant scatter in cluster concentrations, and that the NFW profile is only ‘universal’ in that it fits statistically to isolated clusters, rather than holding in detail for each cluster. We believe that these issues do not have a large effect on determining the cluster normalization (White 2002), however this could be studied in more detail. Careful direct comparison between simulations and observations is probably ultimately the best approach when the next generation of simulations becomes available.

In summary, while both observations and simulations agree quite well on the scaling law of equation (4), there is no obvious agreement on the value of the normalization T_{*} . The observations may favour a higher T_{*} , perhaps 1.8–1.9, while the simulations at present appear to give values around 1.5–1.6. At present it is by no means clear which should be the preferred value, or indeed if they are genuinely discrepant. In what follows, we will investigate the implications on the determination of σ_8 of adopting different M – T assumptions and error treatments.

3.4 Methodology

The general method is similar to the one described in PSW, with some technical improvements. We developed two independent codes for the likelihood evaluation, with slightly different approaches for the treatment of the errors, and we cross-checked the results. This allows us to identify areas of potential disagreement in the σ_8 estimate.

Perhaps the largest modification is that our former Monte Carlo method for the error treatment has been completely replaced by ‘weight functions’ to increase speed. For each set of cosmological parameters, including the normalization and slope of the mass temperature relation, we construct a grid of $n(T)dT$, taking into account the asymmetric nature of the quoted observational errors on the temperatures. At this stage a volume cut based on the L – T relation is applied. A conversion from temperature to mass, and between mass definitions, is used to compare the observed $n(T)$ with theory using the Poisson averaged likelihood

$$\langle \log \mathcal{L} \rangle = \sum_i d_i \log \mu_i - \mu_i, \quad (7)$$

where d_i is the fraction of the cluster in bin i and μ_i is the mean value computed from the mass function and effective volume.

In principle the uncertainty in the mass temperature relation could be treated in two different ways: either with a convolution of the mass function or by marginalising the value of the likelihood. The former approach is appropriate for treating intrinsic scatter, while the latter is more appropriate for an uncertain parameter such as the overall normalization or slope. In PSW we showed that the uncertainty in relating the mass to the observable dominates the final error bar, so it is important to treat this issue as carefully as possible. Both approaches have been adopted in the literature, accordingly, we investigated the influence of the two approaches on the likelihood independently. We also checked that the intrinsic scatter could be treated equivalently through either convolution or by an extended Monte Carlo procedure.

3.5 Results

We present here our results, quoted with respect to a reference model which assumes the HIFLUGCS extended catalogue with temperature from Ikebe et al. (2002). Unless otherwise stated, we will focus on $T_* = 1.75$ and $\Omega_m h = 0.2$. Our fiducial choice for scatter in the M – T relation is 10 per cent in T , with a Gaussian distribution.

We show in Fig. 2 the variation of σ_8 with T_* if we hold $\Omega_m = 0.3$. We find that the uncertainty due to the choice of the fiducial T_* value dominates with respect to the assumed intrinsic scatter. In order for this situation to be improved in future studies, the discrepancy between the observational and simulated T_* values will need to come into better agreement.

In Fig. 3 we show the effect of treating the uncertainty in T_* in two different ways: via convolution of the likelihood function or of the mass function. It is apparent that after marginalisation of the likelihood is performed, the overall effect is to broaden the error bars with respect to the case with no errors. Convolution of the mass function, instead,

mainly shifts σ_8 toward lower values. The two approaches are therefore not equivalent, and should be used appropriately (i.e. convolution or Monte Carlo for the intrinsic scatter and marginalisation for the systematic normalization uncertainty).

These results have been obtained with Gaussian scatter in T . Some authors (e.g. B01) have considered the scatter instead to be Gaussian in $\log(T)$, as observed scaling relations sometimes quote. While there is no particular reason for the latter choice, apart from the convenience of fitting a straight line to the data, we verified that the two different choices give similar error bars, at least at the 1σ level, and for the 10 per cent scatter assumed here. However, we caution that in practice the distribution may not be Gaussian, and the tails may have a disproportionate effect. We also note in Fig. 3 that for relatively small intrinsic error (10 per cent in T) the effect of the scatter is sub-dominant with respect to the other sources of error. However, we see that a 16 per cent scatter is sufficient to shift the σ_8 value by a significant amount.

We show in Fig. 4 the dependence on the assumed mass function. We note here that the results derived with the Jenkins et al. (2001) mass function are more similar to the ones obtained using Press–Schechter (1974) than to those assuming the Sheth & Tormen (1999) form. This is due to the fact that the Jenkins et al. (2001) function is actually closer to Press–Schechter than to Sheth–Tormen in the range $0.3 < \ln \sigma^{-1} < 0.7$ which is mostly relevant here.

The dependence on the specific sample used is shown in Fig. 5. We note that although the cluster sample contains 97 clusters in its extended version, due to our selection criteria the actual number of clusters used is much lower: the code selects on average 28.5 clusters out of the HIFLUGCS sample, 38 out of the extended one and 41.5 out of the old PSW one. About 10 per cent discrepancy between the HIFLUGCS sample and the PSW one is due to the inclusion of the clusters that are nominally below the flux limit (and scatter up from the extended sample). These clusters therefore give a non-negligible contribution to the final σ_8 value through our likelihood technique. The rest of the discrepancy may be explained with the different modeling of the temperatures between Ikebe et al. (2002) and White (2000).

For the dependence of σ_8 on cluster temperature, we verified that cutting out clusters below 4 keV does not result in a significant difference. This means that our 3 keV low temperature cut is high enough to include clusters that actually follow the same M – T relation. We also boosted the temperatures of these clusters above 6.5 keV by 10 per cent, finding no noticeable change in the 90 per cent contour levels. This implies that the level of discrepancy in temperature estimation between, for example, Ikebe et al. (2002) and de Grandi et al. (2002) is probably not a major source of uncertainty.

We also tested the error in the slope of the M – T relation, finding that it is not very important. Increasing the exponent from 1.5 to 1.6 lowers σ_8 by 0.05, while decreasing it to 1.4 increases σ_8 by a similar amount. Since we define our pivot point at $10^{15} h^{-1} M_\odot$, above where most of the sample lies, the sense of the shift is as expected.

Finally, introducing a 35 per cent scatter in the L – T relation when computing volume implies a reduction of about

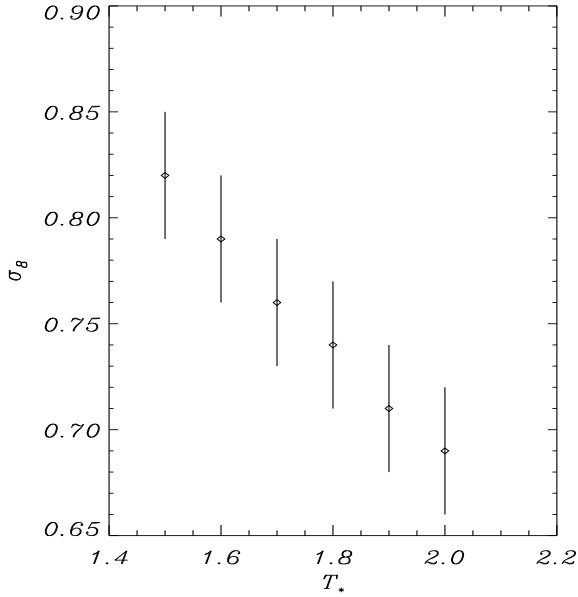


Figure 2. The dependence of σ_8 on the value of the M - T normalization T_* assumed. Here we fix $\Omega_m = 0.3$ and $h = 0.7$. Error bars are 1σ assuming an intrinsic scatter of 10 per cent in T_* . The choice of T_* is probably the most important difference between some discrepant values of σ_8 in the literature.

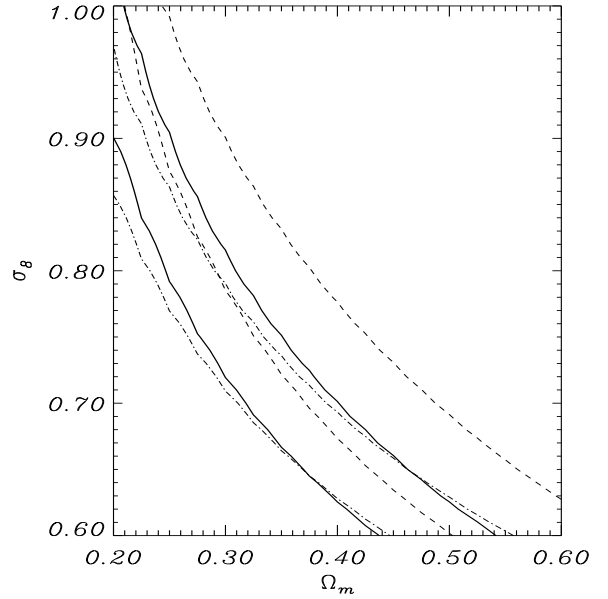


Figure 4. The 90 per cent confidence contours obtained with different mass functions for a fixed $T_* = 1.75$. The solid line corresponds to the Jenkins et al. (2001) mass function in equation (1), the dashed line to that of Sheth & Tormen (1999), and the dot-dashed to the Press & Schechter (1974) formula.

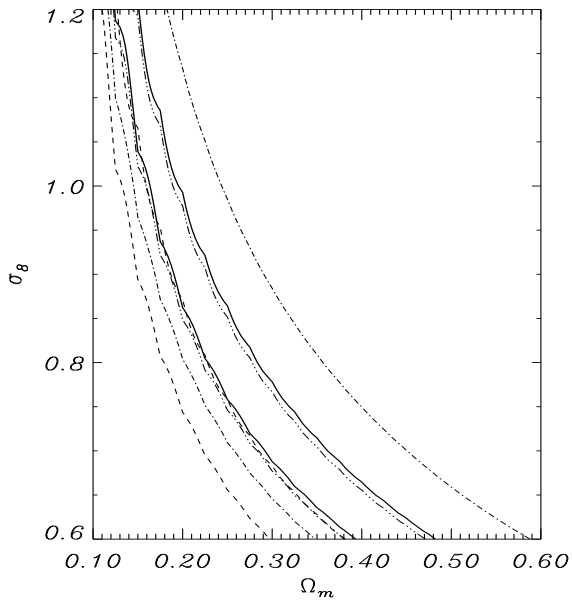


Figure 3. 90 per cent confidence regions in the (σ_8, Ω_M) plane from the analysis of cluster temperatures. The solid contour correspond to a fixed $T_* = 1.75$ (no T scatter), the dot-dashed is obtained by convolving the likelihood function with a 10 per cent error in T , while the three-dots-dashed and dashed are obtained by convolving the mass function with a Gaussian window with a 10 per cent and 16 per cent width in T .

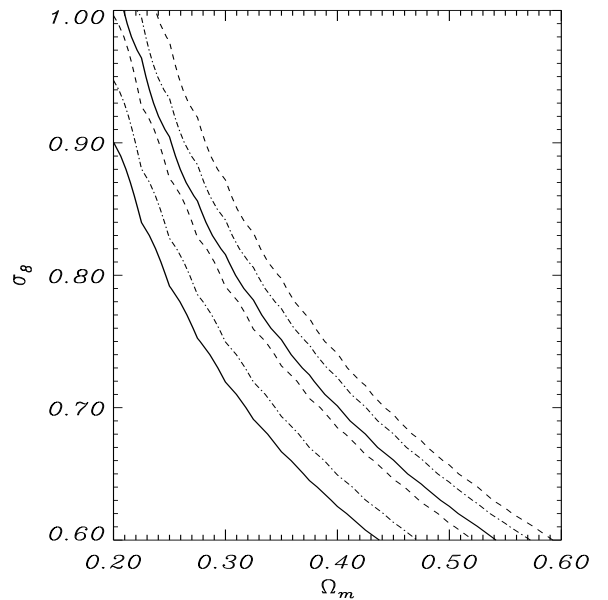


Figure 5. The 90 per cent confidence contours obtained using different input catalogues for a fixed $T_* = 1.75$. The solid line is obtained using the HIFLUGCS sample, the dot-dashed with the extended version (the most appropriate sample to use in our particular methodology), and the dashed with the old PSW catalogue. In the latter case, the L - T relation used is the one from PSW.

8 per cent in the range $4 < T < 8$ keV. However, this has a negligible effect on the final σ_8 result.

After investigating all of these effects, it is clear that one has to be very careful in order to obtain a robust estimate for σ_8 . But even when that has been achieved, the overall error is dominated by the systematic uncertainty in the normalization of the M – T relation.

To obtain an overall ‘best efforts’ estimate for σ_8 we can marginalise over a uniform distribution for T_* , stretching between typical simulation values (1.5) to typical observational values (1.9). For the standard Λ CDM model (with $\Omega_m = 0.3$, $h = 0.7$, $\Omega_b h^2 = 0.02$ and $n = 1$) we obtain

$$\sigma_8 = 0.77^{+0.05}_{-0.04} \quad (8)$$

(c.f. Fig. 2), where the error bars describe the 68 per cent confidence region (corresponding approximately to $\pm 1\sigma$). Here we use our best attempt to construct an effectively temperature-selected sample, which consists of the HI-FLUGCS extended sample (with suitable cuts), plus some additional clusters from PSW. Scalings similar to those given in PSW could be used to extend this to different cosmologies.

4 CONSTRAINTS FROM THE LOCAL XLF

An alternative approach is to dispense with the X-ray temperatures and to use the X-ray luminosity function (XLF). This method suffers from the potential limitation that the relation between X-ray luminosity and mass is less well understood and is more affected by uncertainties in the thermodynamic status of the ICM than the M – T relation. However, the XLF has the significant advantage that it is now precisely calibrated for extended sets of both nearby and distant ($z \sim 1$) cluster samples. Quite remarkably, all the determinations of the local XLF based on the *ROSAT* All Sky Survey (RASS) and on deep pointings agree pretty well with each other (see Rosati, Borgani & Norman 2002, for a review), thus providing a stable reference point to establish the evolution of the X-ray cluster population.

Therefore, it is important to understand the extent to which XTF and XLF approaches give consistent results on cosmological constraints. This is only possible through a careful consideration of the different steps involved. The most recent determination of the local XLF is based on the REFLEX survey (Böhringer et al. 2002, B02 hereafter). This survey includes about 450 clusters out to $z \lesssim 0.3$, and is complete down to the flux limit of $3 \times 10^{-15} \text{ W m}^{-2}$ in the 0.1–2.4 keV energy band. B02 provided a binned representation of the cluster XLF in the luminosity range $L \simeq 4 \times 10^{34}$ to $3 \times 10^{39} \text{ W}$ (with $h = 0.5$) for both an Einstein-de Sitter cosmology and for a flat low-density model with $\Omega_m = 0.3$. The effect of changing cosmology is almost negligible at the low redshifts probed by the REFLEX survey. For definiteness, we will use in the following the XLF determination for the low-density model.

Schuecker et al. (2002) combined clustering properties and redshift distribution of REFLEX clusters, through a maximum-likelihood approach, to obtain constraints on σ_8 and Ω_m . They applied the L – M relation calibrated by RB02 and obtained $\sigma_8 \simeq 0.75$ for $\Omega_m = 0.3$ with formal statistical uncertainties of about 5 per cent. Consistent re-

sults have been also found by Allen et al. (2002), who used the XLF from the REFLEX survey and the BCS (Ebeling et al. 2000), combined with an L – M relation calibrated from *Chandra/ROSAT* data and weak lensing observations. Rather than focusing on a further determination of cosmological constraints from the REFLEX XLF, our analysis is more aimed at understanding how such constraints are affected by the details of the analysis method, and how they compare with those derived from the XTF analysis, presented in the previous section.

Since we use the binned representation of the XLF given by B02, we determine best-fitting values for cosmological parameters and confidence levels by computing the χ^2 between the measured and predicted REFLEX XLF. The model XLF is computed from the mass function of equation (1) by converting masses into observed X-ray luminosities (see below). After finding the values of the (σ_8, Ω_m) parameters which minimize the χ^2 value, confidence regions are estimated from standard 2-dimensional $\Delta\chi^2$ variations. We assume the REFLEX XLF to be determined at the effective redshift $z_{\text{eff}} = 0.1$, which is close to the median redshift of the survey.

4.1 Converting masses into X-ray luminosities

In order to convert the observed L into mass to use in the mass function of equation (1), we follow two different procedures.

4.1.1 Method (a): using L – T and M – T

The first method combines the observed L – T relation and the M – T relation calibrated from hydrodynamical cluster simulations. This procedure has been applied by several authors in the analysis of flux-limited cluster surveys (e.g. Kitayama & Suto 1998, Sadat, Blanchard & Oukbir 1998, Reichart et al. 1999, B01). As for the M – T relation, we use the expression of equation (4).

As for the L – T relation, different analyses consistently show that is well represented at cluster scales ($T \gtrsim 2$ keV) by a power law, $L \propto T^\alpha$, with $\alpha \simeq 3$, and with a scatter which is significantly reduced once the effect of cooling flows has been corrected for (e.g. Markevitch 1998, Allen & Fabian 1998) or by considering only systems without significant cooling-flow signatures (e.g. Arnaud & Evrard 1999). Following the same notation for the relation between bolometric luminosity and emission-weighted temperature as in B01, the expression we use is

$$L_{\text{bol}} = L_6 (T/6 \text{ keV})^\alpha 10^{37} h^{-2} \text{ W}, \quad (9)$$

with $L_6 = 3$ and $\alpha = 3$. Bolometric luminosity is then converted into the 0.1–2.4 keV band by using a MEKAL spectral synthesis code, assuming one-third solar metallicity for the intra-cluster medium. Since this conversion has a larger effect for hotter systems, the L – T relation tends to flatten when computed in the 0.1–2.4 keV band. This is the reason for the different slopes in equations (3) and (9). We assume that the combination of M – T and L – T variation results in an overall 45 per cent scatter, which is assumed to be Gaussian-distributed in the log.

4.1.2 Method (b): using $M-L$ directly

The second method uses an observationally determined $M-L$ relation (RB02, Ettori et al. 2002). RB02 estimated the $M-L$ relation for a sample of 103 clusters with $L \gtrsim 10^{35} h_{50}^{-2} \text{W}$, temperature measured from ASCA and gas density profiles from ROSAT PSPC pointed observations. Ettori et al. (2002) used *Beppo-SAX* data for a set of 22 clusters with $T > 3$ keV, with measured profiles of gas temperature and density. Based on such data, they found that, unlike for the $L-T$ relation, no segregation between cooling-flow and non cooling-flow clusters exists in the $M-L$ plane. As a consequence, these authors claim that directly measuring the $M-L$ relation is more stable than combining the $L-T$ and $M-T$ relations.

In the following, we will use the $M-L$ relation from RB02, which includes lower-luminosity systems, thus better covering the L range probed by the REFLEX XLF. We consider the relation based on mass estimated at overdensity $\Delta = 500$ and luminosity in the 0.1–2.4 band. As in Section 3.3, M_{500} will be related to $M_{\Delta c}$ assuming an NFW profile with $c = 5$ for the concentration parameter. RB02 claims that no extrapolation is required for 86 per cent of the clusters in their sample to obtain mass at such an overdensity (although obviously the assumption of a $c = 5$ NFW profile is still required to connect M_{500} to $M_{180\text{m}}$). RB02 adopted a fitting expression of the form $L = 10^A (M_{500}/h_{50}^{-1} M_{\odot})^{\alpha} h_{50}^{-2} 10^{33} \text{W}$ and provided fitting parameters for both the direct ($A = -19.708$, $\alpha = 1.652$) and inverse relations ($A = -17.545$, $\alpha = 1.504$; see Table 10 in RB02). In the following we will show results based on these different choices for A and α , so as to judge the stability of constraints on cosmological parameters against uncertainties in the fitting procedure.

Finally, RB02 also estimated the overall scatter in mass from this relation to be $\simeq 48$ per cent. After subtracting in quadrature the contribution from the mean mass measurement uncertainty, $\simeq 28$ per cent, the resulting intrinsic scatter in the $M-L$ relation turns out to be 39 per cent. This value overestimates the true scatter if errors in the mass measurements have been underestimated, for instance due to the assumptions of isothermal gas and β -model fitting for the gas density profile, made by RB02 in their analysis. Also, if significant temperature gradients are present (e.g. Markevitch et al. 1998, Finoguenov et al. 2001, De Grandi & Molendi 2002, Pratt & Arnaud 2002), then the isothermal assumption would lead to an overestimate of the total gravitating mass and, therefore, to an overestimate of σ_8 at fixed Ω_m . Whether violations of these assumptions would lead to a bias or to an increase in the scatter or both is unclear.

Following the same line of reasoning as in Section 3.4 for the $M-T$ relation, any uncertainty in the $M-L$ relation can be interpreted as due either to a genuine intrinsic scatter or to an overall uncertainty in the normalization of the relation. In the first case, one has to convolve the model mass function with a scatter, while in the second case the correct procedure is to marginalise over the amplitude of the $M-L$ relation, after assuming a range of variation and a distribution for this parameter. In the following we will assume as our fiducial analysis that based on the RB02 $M-L$ relation, with 20 per cent intrinsic scatter in mass. We will also verify how the

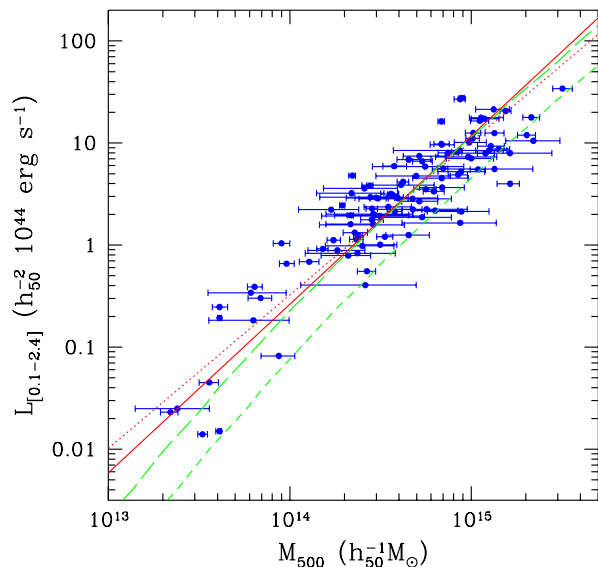


Figure 6. The relation between M_{500} and luminosity in the 0.1–2.4 keV energy band. Data points are from Reiprich & Böhringer (2002, RB02). Solid and dotted lines represent the direct and inverse best-fitting relations from RB02. Long-dashed and short-dashed lines have been obtained from the combined $L-T$ and $T-M$ method to convert mass into L , after assuming $T_* = 1.75$ and $T_* = 1.2$, respectively. We assume $\Omega_m = 0.3$ and use equation (4) for the $M-T$ conversion. Bolometric luminosities have been converted into L in the 0.1–2.4 keV band by using a MEKAL model with $Z = 0.3 Z_{\odot}$ for the ICM metallicity.

results change by marginalising over the amplitude of the $M-L$ relation and by changing the intrinsic scatter between the two extreme assumptions of negligible scatter and 39 per cent scatter. We show in Fig. 6 the observational data points from RB02 along with the different $M-L$ relations that we use in our analysis. Method (a) with $T_* = 1.2$ (used by B01) overestimates the mass at a fixed luminosity, while taking $T_* = 1.75$ is rather close to the fitting relations used by RB02 for $L \gtrsim 10^{36} \text{W}$.

4.2 Results

From their analysis of the ROSAT Deep Cluster Survey (RDCS), B01 derived constraints on the (Ω_m, σ_8) plane by following the evolution of the cluster population out to $z \gtrsim 0.8$ (see also Rosati et al. 2002). This analysis was based on the combined $L-T$ and $T-M$ approach of method (a) with $T_* = 1.2$, no significant evolution of the $L-T$ relation (e.g. B01, Holden et al. 2002, Novicki, Sornig & Henry 2002; cf. also Vikhlinin et al. 2002), an overall 45 per cent scatter in the $M-L$ relation, and assuming the mass function by Sheth & Tormen (1999).

For the sake of direct comparison, we repeat here the same analysis on the REFLEX XLF. We emphasize that a major difference between the analysis of RDCS and of REFLEX lies in the widely different volumes covered by the two surveys at different redshifts – unlike REFLEX, the RDCS has a modest volume coverage at low redshift, while being

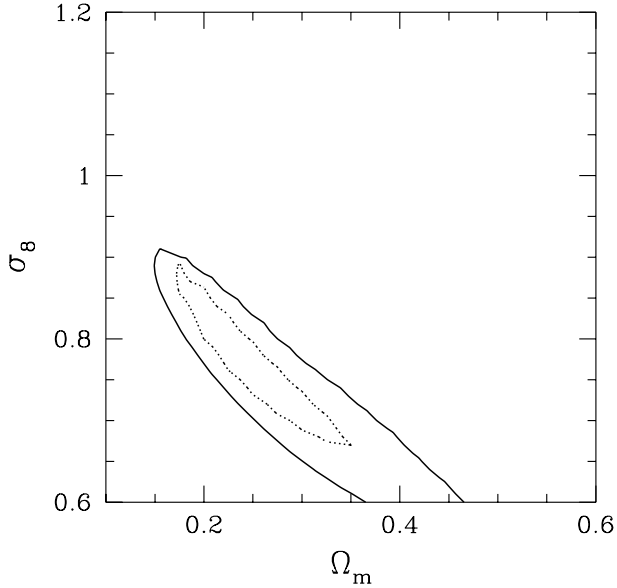


Figure 7. Comparison between the constraints derived from the REFLEX and the RDCS XLF. The solid contour indicates the 90 per cent confidence region from the REFLEX XLF, by using the method (a) for the mass–luminosity conversion (Section 4.1.1), with L – T relation given by equation (9), M – T relation by equation (4) with $T_* = 1.2$. The dotted contour corresponds to the analysis of the evolution of the RDCS XLF out to $z \simeq 0.8$ (B01, Rosati et al. 2002; see text), for the same choice of L – T and M – T relations and assuming a non-evolving L – T (for $\Omega_m = 1.0$). In both analyses the mass function is convolved with 45 per cent scatter in the overall M – L conversion. For the sake of comparison with the results of B01, we used here a BBKS power spectrum with $\Gamma = 0.2$ for the shape parameter and the mass function by Sheth & Tormen (1999).

able to trace the cluster population out to $z \sim 1$. Therefore, the analysis of the RDCS provides a *dynamical* constraint on Ω_m , by probing the growth rate of density perturbations, while REFLEX provides a *geometrical* constraint on Ω_m through the shape of the power spectrum (assuming CDM and fixing h and Ω_b from independent observations).

We compare in Fig. 7 the constraints from REFLEX and RDCS. Quite remarkably such constraints are in good agreement. The somewhat looser constraints from REFLEX should be understood in terms of the largely different nature of the two samples, which cover widely different redshift ranges, and of the different analysis method – the RDCS analysis is based on a maximum likelihood approach, which allows one to extract the whole information provided by the distribution of clusters in the L – z plane. Besides the values of σ_8 , the agreement between the ‘geometrical’ and ‘dynamical’ measurements of Ω_m is quite remarkable. We believe that this finding represents important support for the reliability of using galaxy clusters as tracers of the evolution of cosmic structures.

We show in Fig. 8 how cosmological constraints alter as we change different aspects of the analysis procedure, such as the M – L conversion, as well as the amount of uncertainty in this conversion and how it is treated. Our reference analysis corresponds to choosing the best-fitting direct M – L relation

from RB02, with 20 per cent intrinsic scatter, convolved with the mass function (results shown with solid contours in the panels). In this case, we obtain

$$\sigma_8 = 0.86_{-0.16}^{+0.12}; \Omega_m = 0.23_{-0.06}^{+0.10}, \quad (10)$$

where error bars correspond to 68 per cent uncertainties on the two parameters. If we fix the density parameter at $\Omega_m = 0.3$, we find

$$\sigma_8 = 0.74_{-0.04}^{+0.03}, \quad (11)$$

where the error corresponds to the 68 per cent uncertainty for one interesting parameter. The above quoted errors only reflect the shot noise, propagated from the Poissonian errors quoted by B02 (and no systematic uncertainty in the M – L relation, which we discuss below). As pointed out by Evrard et al. (2002; see also Hu & Kravtsov 2002 and White 2002), sample variance due to finite survey size and clustering should also be considered. However, given the large size of the REFLEX survey, we expect sample variance not to be important, compared with other uncertainties related to the M – L conversion.

In the left panel of Fig. 8 we show the effect of changing the amount of intrinsic scatter in the M – L relation. As expected, assuming a larger scatter decreases the normalization of the power spectrum. For instance, taking $\Omega_m = 0.3$ and assuming zero scatter gives $\sigma_8 \simeq 0.8$, while assuming a 39 per cent scatter lowers σ_8 to about 0.65. In the central panel we show the effect of the statistical uncertainty in the M – L relation, by considering both the direct and the inverse fitting provided by RB02, as well as the effect of marginalising the likelihood over the M – L amplitude. The effect of using the inverse fitting (dotted contour) is that of marginally favouring lower Ω_m values, while keeping the σ_8 – Ω_m degeneracy direction unchanged. This indicates that the statistical stability of the M – L conversion has only a small effect. As for the marginalisation procedure (thin continuous contour), it has been realized by integrating the likelihood function over a range of M – L amplitudes, defined by varying the best-fitting value by ± 20 per cent, with a uniform distribution. The effect of marginalising is that of widening the contours, while shifting the most likely σ_8 to larger values, since no convolution with the scatter is now performed. In fact, for $\Omega_m = 0.3$ we have

$$\sigma_8 = 0.79_{-0.07}^{+0.06}, \quad (12)$$

for the 68 per cent confidence region.

The right panel shows the effect of using method (a) for the M – L conversion, and assuming $T_* = 1.75$, as a compromise between observational and theoretical determinations. Since the M – L relations from these two methods are quite similar (see Fig. 6), the slightly higher normalization from method (b) is precisely the consequence of having assumed a 20 per cent intrinsic scatter, instead of 45 per cent as in method (a).

5 DISCUSSION

5.1 Comparing XTF and XLF results

We can now compare the XLF and XTF approaches, making as far as is possible consistent assumptions throughout.

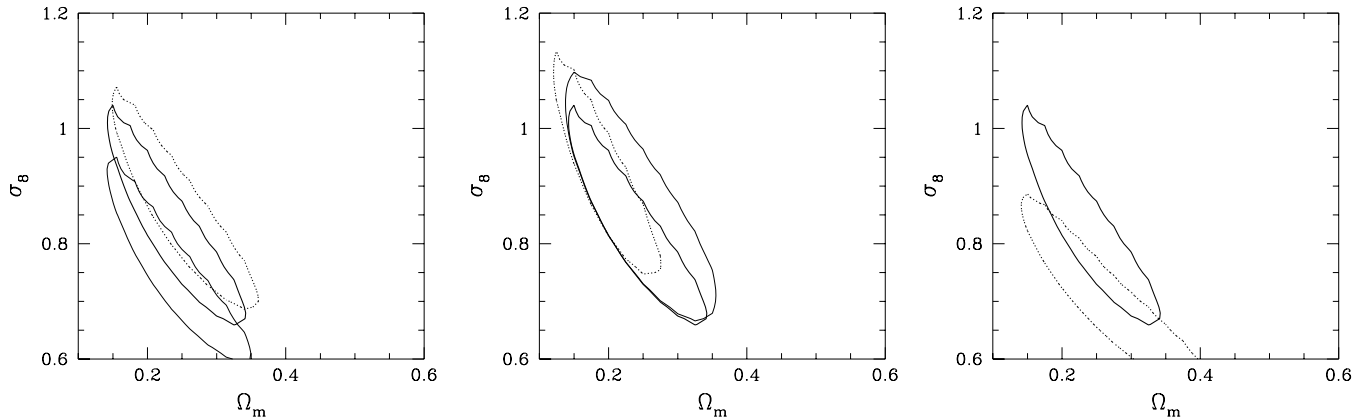


Figure 8. The 90 per cent confidence contours for the REFLEX XLF, for different choices of the $M-L$ conversion. In all panels, the solid contour corresponds to the reference analysis method, taking the best-fitting direct $M_{500}-L$ conversion by Reiprich & Böhringer (2002, RB02) and convolving the model mass function with 20 per cent intrinsic scatter. Left panel: the dotted contour is for the effect of assuming no intrinsic scatter in the $M_{500}-L$ relation by RB02, while the thin continuous contour is for the maximal assumption of 39 per cent intrinsic scatter in the $M_{500}-L$ relation. Central panel: the thin continuous contour shows the effect of marginalising over the amplitude of the $M-L$ relation, which is assumed to vary with a uniform distribution of ± 20 per cent about the best-fitting value; the dotted contour is based on taking the inverse $M-L$ best-fitting parameters, as provided by RB02, in the reference analysis. Right panel: the dotted contour is for the $M-L$ conversion based on the same method used to obtain the solid contour in Fig. 7, but with $T_* = 1.75$ for the $M-T$ relation (long-dashed line in Fig. 6).

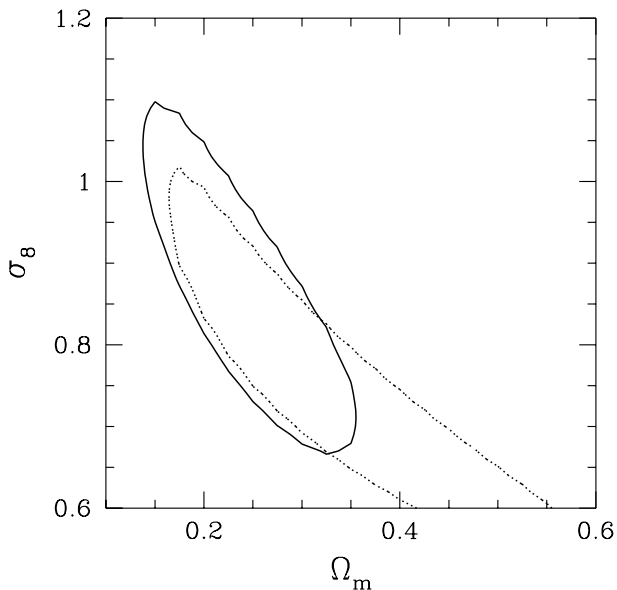


Figure 9. Comparison between the 90 per cent confidence contours derived from the REFLEX XLF (continuous line) and the XTF analysis (dotted line). The XLF analysis is based on method (b) for the $M-L$ conversion, by marginalising over the amplitude of the $M-L$ relation by RB02, which is varied by ± 20 per cent around the best fitting value with uniform distribution (see text). The XTF contour has been obtained by marginalising over T_* , which is assumed to vary with uniform distribution from 1.5 to 1.9 (see also eq.10). Both analyses are based on assuming $\Omega_b = 0.019 h^{-2}$ and $h = 0.7$ in the power spectrum by Eisenstein & Hu (1999).

We show in Fig. 9 a comparison between the marginalised constraints derived from the analyses of the previous sections. Both analyses have been realized by assuming $\Omega_b = 0.019 h^{-2}$ and $h = 0.7$ in the power spectrum by Eisenstein & Hu (1999). The XLF constraint is that derived by marginalising over the amplitude of the $M-L$ relation by RB02, on which the result of eq.(15) is based. The XTF result is derived by marginalising over T_* , which is uniformly varied from 1.5 to 1.9. Even bearing in mind the systematics affecting both the XTF and the XLF analyses, the two methods provide remarkably consistent constraints. This represents a non-trivial result, owing to the quite different approaches by which such constraints have been derived: not only are the cluster samples and the analysis methods different, but also the systematics associated with the $M-T-L$ scalings enter in completely independent ways. Although different assumptions on how to interpret and treat the scatter in the $M-T$ and $M-L$ relations produce different XLF- and XTF-based constraints, nevertheless it is reassuring that such a good agreement is just obtained for rather natural choices of these parameters. The wider contour from the XTF analysis is due to the narrower dynamical range probed in cluster masses by our sample of cluster temperatures, which does not allow to put strong constraints on the shape of the power spectrum. In fact, while our XTF samples about half a decade in temperature, the REFLEX XLF samples about 3.5 decades in cluster luminosity (0.1-2.4 keV band), which correspond to almost 1.5 decades in temperature from the $L-T$ relation of eq.(3).

The main disagreement between the XTF analysis by PSW and the XLF analysis by B01 was neither due to the reliability of one of the two or both samples, nor to the T_* assumed (which in fact would have implied a discrepancy in the opposite direction), but rather to the procedure of convolving versus marginalising the scatter. This illustrates that

although the application of the cluster abundance normalization technique appears to be simple, it involves a chain of steps, and the source of discrepancies can be rather subtle. However it also serves to reinforce our central point – with sufficient care the statistical and methodological differences can be reduced to the point that the major remaining uncertainty is in the normalization of the mass scale of clusters and in the determination of the nature of the scatter between the theory–predicted mass and the observed X–ray luminosity and temperature.

5.2 Comparing with other estimates of σ_8

We list in Table 1 other recent determinations of σ_8 , which are based on different methods. Older estimates and associated references can be found in PSW. Rather than analyse individual studies in detail, we will make some general remarks which help explain the differences.

The normalization of density perturbations (through the mass variance at $8 h^{-1} \text{Mpc}$) can be evaluated by means of several different observables, either on much larger scales (e.g. CMB derived constraints), on scales $\sim 10 h^{-1} \text{Mpc}$ (containing the mass of a rich cluster of galaxies, which is not far into the non-linear regime), or on much smaller scales (e.g. through lensing or Ly α forest variance measurements). Normalization estimates from large or small scales can be interpreted as σ_8 determinations through extrapolation of the power spectrum. This is cosmology dependent, and hence it should be no surprise that some of the estimates in Table 1 appear discrepant. Even if we focus on methods which are directly measuring the mass variance on scales close to $8 h^{-1} \text{Mpc}$, there still appears to be a bewilderingly wide range of published values.

One point to realize is that different cosmological assumptions are made by different sets of authors. Since the density parameter is constrained to a first approximation through the combination $\Omega_m h$ (sometimes referred to as the ‘shape parameter’), any uncertainty in the value of h translates into a similar uncertainty when constraining Ω_m . Hence there are ambiguities here, which one has to be careful about when comparing results between authors. Different values of σ_8 will be obtained using identical data but either a fixed h , fixing $\Omega_m h$, or marginalising over various priors. This explains some of the discrepancies in the Table.

There have been several recent results from weak lensing (Bacon et al. 2002, Brown et al. 2002, Hoekstra et al. 2002, Jarvis et al. 2002, Refregier et al. 2002, van Waerbeke et al. 2002). The quoted σ_8 values, reported in Table 1 in chronological order, range between 0.7 and 0.9, and have been decreasing in the past year. It is early days for this method, since the formal significance of cosmic shear detection is still rather modest. More importantly for the purposes of comparison with cluster abundance values of σ_8 , most lensing studies have only poor knowledge of their source redshift distributions and are measuring on a scale which is a factor of several smaller than the $\sim 10 h^{-1} \text{Mpc}$ probed by clusters, and may be affected by non-linear clustering. Despite the fact that latest works have done major improvements in assessing systematic error via the B–mode power spectrum, this still remains a very hard measurement and the nature of the systematic errors is not yet well understood. Estimates using large-scale structure measurements

coupled with Cosmic Microwave anisotropies (e.g. Lahav et al. 2001) also give similar values, but are even more dependent on the adopted cosmology and which parameters are held fixed.

There are many other minor differences between some of the studies involving the analysis of the cluster number density. Precisely how the samples are constructed is obviously a major issue. For instance, when dealing with X-ray properties this is particularly an issue for deciding how best to deal with substructure and cooling flows. Here different authors make different decisions, and it is to be hoped that such ambiguities will eventually disappear as the simulations improve and can be more directly compared with the observations. Another issue is merging corrections, which some recent studies have used, motivated by the idea that Press-Schechter describes the number density of halos at the virialisation epoch. However (as we stressed in PSW), it is clear that the effect of merger history is already implicit in the intrinsic scatter of the M – T relation, and so should not be included twice. Other minor issues include whether redshift corrections are made, what profiles are used to convert between different mass quantities, whether there is curvature in the adopted M – T or M – L relations, etc.

To summarize this part: differences in σ_8 can be due to a number of factors. Firstly, the method used may require an extrapolation to $8 h^{-1} \text{Mpc}$. Secondly, there are varying assumptions made about the values of other cosmological parameters in the analysis. Thirdly, there are different forms used for the mass function or the transfer function. Fourthly, even when the basic method adopted is the same, there can still be detailed differences in the approaches of each set of authors (e.g. which sources of scatter are included, how the catalogue is constructed or whether a merger correction is applied). And finally, for XTF- and XLF-based approaches there is the choice for the mass–temperature and mass–luminosity conversion, respectively.

6 CONCLUSIONS

We investigated the determination of σ_8 as derived from the XTF and XLF approaches. We considered many possible choices in terms of data and methodology, and paid special attention to the assessment of possible sources of biases and systematic uncertainties in the adopted procedure.

In both XTF- and XLF-derived constraints, the most important effect on σ_8 estimates is the error in the scaling relation connecting mass to temperature and to luminosity. Moreover, different ways of introducing such an error have a significant impact on the final σ_8 range. If it is introduced as a convolution with the mass function, its overall effect is to lower the σ_8 value, while if it is introduced by marginalising the final likelihood, then the consequence is mainly to broaden the error contours. We argue that the former (latter) procedure is more adequate when dealing with statistical (systematic) errors. For instance, in the marginalisation procedure one has to make a decision about the functional form of the distribution with which the marginalised parameters are varied. In our comparison between XTF- and XLF-based constraints (see Fig. 9) we decided to assume a uniform distribution for T_* within a finite range. While there is no rigorous justification for this choice, this pro-

Authors	σ_8	error	Γ	Method
Van Waerbeke et al. (2001)	0.88	0.05	–	WL
Van Waerbeke et al. (2002)	0.98	0.06	0.2	WL
Bacon et al. (2002)	0.97	0.13	–	WL
Refregier et al. (2002)	0.93	0.17	0.21	WL
Hoekstra et al. (2002)	0.87	0.03	–	WL
Brown et al. (2002)	0.74	0.09	–	WL
Hamana et al. (2002)	0.73	0.27	0.21	WL
Jarvis et al. (2002)	0.71	0.14	0.21	WL
Bahcall et al. (2002)	0.72	0.06	–	OC
Viana et al. (2002)	0.61	0.10	0.1	WLC
Blanchard et al. (2000)	0.75	0.02	–	XTF
Henry (2000)	0.77	0.15	–	XTF
Oukbir & Arnaud (2001)	0.91	–	–	XTF
Pierpaoli et al. (2001)	1.02	0.07	0.23	XTF
Seljak (2001)	0.77	0.06	0.20	XTF
Reiprich & Böhringer (2002)	0.68	0.13	0.17	XLF
Borgani et al. (2001)	0.67	0.06	0.23	XLF
Schuecker et al. (2002)	0.71	0.03	–	XLF
Allen et al. (2002)	0.72	0.02	–	XLF
Lahav et al. (2001)	0.73 – 0.83	0.07	0.21	PS
Szalay et al. (2001)	0.91	0.06	0.19	PS
Bond et al. (2002)	≥ 1	–	–	SZ PS
Komatsu & Seljak (2002)	1.05	0.05	–	SZ PS

Table 1. Some recent estimates of σ_8 . The errors are typically statistical. We have tried to give values consistently for $\Omega_m \simeq 0.3$, while $\Gamma \simeq 0.2$ is a typical value of the shape parameter. Methods used include: weak lensing (WL); Optical clusters (OC); clusters normalized using weak lensing (WLC); X-ray temperature function (XTF); power spectrum (PS); Sunyaev-Zel’dovich effect power spectrum (SZ). The two errors for the WL analysis by Refregier et al. (2002) are for statistical uncertainty and cosmic variance, respectively.

cedure allowed us to have hints about the effect of treating the uncertainties in the L – T – M scaling relations in different ways. On the other hand, in order to treat errors adequately, one should be able to precisely assess their nature, and at the moment the split between scatter and overall normalization uncertainties is not well characterised, nor are these uncertainties precisely quantified. We notice, for example, that part of the previous disagreement between PSW and B01 was not in fact due to the adopted value of the M – T normalization T_* (which would have given a discrepancy in the opposite direction), but rather to the statistical procedure used.

For the XTF approach, the main scaling relation involved is the M – T one. Despite the fact that the agreement between observations and simulations has improved, mainly due to better modeling of the cluster physics in the simulations (e.g. Muanwong et al. 2002; Davé et al. 2002; Tornatore et al. 2002, in preparation), there is still a significant scatter in the quoted T_* values. Should that be taken as the ‘systematic’ error, it would certainly dominate the statistical error quoted by either observers or simulators (which is typically about 10 per cent). At the same time, observational mass determinations are probably affected by significant biases, due for instance to the necessary extrapolation from the (small) internal region observed to the larger one involved in the mass function. Other source include possible deviations of the surface brightness profile from simplified fitting models and to the violation of the often made hydrostatic and isothermal assumptions.

The same general comments apply to the XLF approach. In this case, the fairly large number of clusters included in nearby and distant samples means statistical noise

is unimportant for the resulting uncertainties. In fact the same complex physical processes which affect the ICM temperature are also very important when dealing with X-ray luminosity, which is highly sensitive to the local properties of the ICM. Therefore, more robust constraints on σ_8 will require substantial efforts to improve both the observational picture and the theoretical understanding of the relevant physical processes, which determine the X-ray properties of the intra-cluster medium.

Because of the variety of σ_8 values in the literature, we carried out careful tests of the impact of different assumptions on the final result. On the theoretical side, it is important to rely on the most accurate mass function for the model being considered. In our analysis, we have used the Jenkins et al. (2001) mass function, and found that it gives closer results to pure Press–Schechter than to Sheth–Tormen for the mass range probed. Moreover, the use of the explicit σ_8 quantity instead of fitting formulae, as well as an accurate transfer function which properly includes baryonic suppression, is also necessary in order to reach the desired accuracy. While such effects are probably small with respect to the systematic uncertainties in the M – T – L relations, nevertheless they should be properly understood if the cluster abundance normalization is to be determined with high precision.

Bearing in mind all these caveats, a few firm conclusions can be drawn from our analysis. Firstly, current data on the XLF and XTF for nearby clusters give quite consistent results on cosmological parameters, with $\sigma_8 \simeq 0.8$ for a flat $\Omega_m = 0.3$ Universe. While one would be tempted to attach a ~ 5 per cent statistical error (at 1σ) to this determination, it is fair to say that at least twice as large an error, associated

with uncertainties in the $M-T$ and, especially, in the $M-L$ relations, is more realistic. Secondly, under the same assumptions for the $M-L$ conversion in the XLF analysis, dynamical constraints on the (Ω_M, σ_8) plane, derived from the evolution of the cluster population (e.g. B01), are fully consistent with the geometrical constraints derived from nearby samples.

The cluster abundance as a cosmological probe has been developing very fast in the past few years. New observations have allowed an empirical determination of the scaling relations involved, while more refined simulations are helping to reconcile past discrepancies with observations. Furthermore, great effort has been devoted in understanding which modelling should be used in terms of transfer and mass function, and to the statistical procedures to compare observed and predicted number density of galaxy clusters. Further improvements are expected also on the observational side, thanks to the improved capability of X-ray satellites of the last generation to precisely measure cluster temperatures. A careful study over a statistically significant sample of cluster will therefore allow a better calibration of the scaling relations and of their intrinsic scatter. At the same time, improvements in simulations, in terms of both resolution and physics included, will allow a reliable framework for the interpretation of the observational results.

X-ray surveys, both in contiguous areas and based on cluster searches from *Chandra* and *XMM* archives, will certainly help in improving the quantity and quality of cluster data. Future surveys, using missions like *WFXT* (Burrows et al. 1992) or *DUET*, as well as Sunyaev-Zel'dovich surveys (see Table 1 of Schulz & White 2002 for a list), will be extremely valuable for increasing the statistics of clusters at $z > 1$ by orders of magnitude, to enable evolutionary studies to be carried out. However, what is really needed is a robust set of mass estimates for a sample of clusters. An inter-comparison of multi-wavelength mass estimates, from X-ray data, velocity dispersions, gravitational lensing and Sunyaev-Zel'dovich measurements should enable systematic biases to be much better understood than they are at the moment. On the theoretical side, the challenge for the future will be to realize a new generation of cluster simulations, where the inclusion of the relevant physical processes should be coupled with a large enough dynamical range so as to accurately resolve the internal structure of the clusters while encompassing cosmological volumes. It will require a concerted effort from both the theoretical and observational communities, tackling the many remaining obstacles, in order to hone the cluster abundance into a precision cosmological tool and to keep it competitive with rapid advances in the other methods.

ACKNOWLEDGMENTS

EP is supported by NASA grant NAG5-11489, DS by NSERC-Canada and MW by NSF, NASA, DoE and a Sloan Foundation Fellowship. The authors wish to thank Hans Böhringer, Luigi Guzzo, George Ellis, Vincent Eke, Piero Rosati and Peter Schuecker for helpful and stimulating discussions. EP and MW are grateful to the Aspen Center for Physics and to the KITP for hospitality during the preparation of this work; EP is also grateful to the ‘Dipartimento

di Astronomia di Trieste’ and DS is grateful to the Institute for Astronomy, Edinburgh.

REFERENCES

- Allen S.W., Fabian A.C., 1998, *MNRAS*, 297, L57
 Allen S.W., Schmidt R.W., Fabian A.C., 2001, *MNRAS*, 328, L37
 Allen S.W., Schmidt R.W., Fabian A.C., Ebeling H., 2002, *MNRAS*, submitted, astro-ph/0208394
 Arnaud M., Evrard A.E., 1999, *MNRAS*, 305, 631
 Bacon D., Massey R., Refregier A., Ellis R., 2002, *MNRAS*, submitted, astro-ph/0203134
 Bardeen J.M., Bond J.R., Kaiser N., Szalay A.S., 1986, *ApJ*, 304, 15
 Blanchard A., Sadat R., Bartlett J.G., Le Dour M., 2000, *A&A*, 362, 809
 Böhringer H., et al., 2002, *ApJ*, 566, 93 (B02)
 Borgani S., et al., 2001, *ApJ*, 561, 13 (B01)
 Brown M.L., Taylor A.N., Bacon D.J., Gray M.E., Dye S., Meisenheimer K., Wolf C., 2002, *MNRAS*, submitted, astro-ph/0210213
 Burrows C.J., Burg R., Giacconi R., 1992, *ApJ*, 392, 760
 Davé R., Katz N., Weinberg D.H., 2002, *ApJ*, 579, 23
 De Grandi S., Molendi S., 2002, *ApJ*, 567, 163
 Ebeling H., Edge A.C., Allen S.W., Crawford C.S., Fabian A.C., Huchra J.P., 2000, *MNRAS*, 318, 333
 Eke V.R., Cole S., Frenk C.S., Henry J.P., 1998, *MNRAS*, 298, 1145
 Eisenstein D.J., Hu W. 1999, *ApJ*, 511, 5
 Ettori S., De Grandi S., Molendi S., 2002, *A&A*, 391, 841
 Evrard A.E., et al., 2002, *ApJ*, 573, 7
 Evrard A.E., Metzler C.A., Navarro J.F., 1996, *ApJ*, 469, 494
 Finoguenov A., Arnaud M., David L.P., 2001, *ApJ*, 555, 191
 Finoguenov A., Reiprich T.H., Böhringer H., 2001, *A&A*, 368, 749
 Hamana T., et al., 2002, *ApJ*, submitted, astro-ph/0210450
 Henry J.P., 2000, *ApJ*, 534, 565
 Henry J.P., Gioia I.M., Maccararo T., Morris S.L., Stocke J.T., Wolter A., 1992, *ApJ*, 386, 408
 Hoekstra H., Yee H.K.C., Gladders M.D., Barrientos L.F., Hall P.B., Infante L., 2002, *ApJ*, 572, 55
 Holden B.P., Stanford S.A., Rosati P., Squires G., Tozzi P., FSBury R.A.E., Papovich C., 2001, *AJ*, 124, 33
 Horner D.J., Mushotzky, R.F., Scharf C.A., 1999, *ApJ*, 520, 78
 Hu W., Kravtsov A.V., 2002, *ApJ*, submitted, astro-ph/0203169
 Huterer D., White M., 2002, *ApJL*, 578, L95
 Ikebe Y., Reiprich T.H., Böhringer H., Tanaka Y., Kitayama T., 2002, *A&A*, 383, 773
 Jenkins A., Frenk C.S., White S.D.M., Colberg J.M., Cole S., Evrard A.E., Yoshida N., 2001, *MNRAS*, 321, 371
 Jarvis M., Bernstein G., Jain B., Fisher P., Smith D., Tyson J.A., Wittman D., astro-ph/0210604
 Kitayama T., Suto Y., 1997, *ApJ*, 490, 557
 Lahav O., et al., 2002, *MNRAS*, 333, 961
 Levine E.S., Schulz A.E., White M., 2002, *ApJ*, 577, 569
 Markevitch M., 1998, *ApJ*, 504, 27
 Muanwong O., Thomas P.A., Kay S.T., Pearce F.R., 2002, *MNRAS*, 336, 527
 Metzler C.A., White M., Loken C., 2001, *ApJ*, 547, 560
 Nevalainen J., Markevitch M., Forman W.R., 2000, *ApJ*, 532, 694
 Novicki M.C., Sornig M., Henry J.P., 2002, *AJ*, 124, 2413
 Oukbir J., Blanchard A., 1992, *A&A*, 262, L21
 Oukbir J., Arnaud, M., 2001, *MNRAS*, 326, 453
 Pen U.-L., 1998, *ApJ*, 498, 60
 Pierpaoli E., Scott D., White M., 2001, *MNRAS*, 325, 77 (PSW)

- Pratt G.W., Arnaud M., 2002, A&A in press, preprint astro-ph/0207315
- Press W.H., Schechter P., 1974, ApJ, 193, 437
- Refregier A., Rhodes J., Groth E.J., 2002, ApJ, 572, L131
- Reichart D.E., Nichol R.C., Castander F.J., Burke D.J., Romer A.K., Holden B.P., Collins C.A., Ulmer M.P., 1999, ApJ, 518, 521
- Reiprich T., Böhringer H., 2002, ApJ, 567, 716 (RB02)
- Rosati P., Borgani S., Norman C., 2002, ARAA, 40, 539
- Sadat R., Blanchard A., Oukbir J., 1998, A&A, 329, 21
- Schuecker P., Böhringer H., Collins C.A., Guzzo L., 2002, A&A, submitted, astro-ph/0208251
- Schulz A., White M., 2002, ApJ, in press, astro-ph/0210667
- Seljak U., 2001, MNRAS, submitted (preprint astro-ph/0111362)
- Sheth R.K., Tormen G., 1999, MNRAS, 308, 119
- Thomas P.A., Muanwong O., Kay S.T., Liddle A.R., 2002 MNRAS 330, L48
- Trümper J., 1993, Science, 260, 1769
- Van Waerbeke L., et al., 2001, A&A, 374,757
- Van Waerbeke L., Mellier Y., Pello R., Pen U.-L., McCracken H.J., Jain B., 2002, A&A, 393, 369
- Viana P.T.P., Nichol R.C., Liddle A.R., 2002, ApJ, 569, L75
- Vikhlinin A., VanSpeybroeck L., Markevitch M., Forman W.R., Grego L., 2002, ApJ, 578, L107
- White D., 2000, MNRAS, 312, 663
- White M., 2001, A&A, 367, 27
- White M., 2002, ApJS, 143, 241
- Wu J.-H.P., 2001, MNRAS, 327, 629
- Xu H., Jin G., Wu X.-P., 2001, ApJ., 553, 78